

VICReg: Variance-Invariance-Covariance Regularization for Self-Supervised Learning

Adrien Bardes^{1,2}

Jean Ponce^{2,4}

Yann LeCun^{1,3,4}

¹Facebook AI Research

²Inria, École normale supérieure, CNRS, PSL Research University

³Courant Institute, New York University

⁴Center for Data Science, New York University

Abstract

Recent self-supervised methods for image representation learning are based on maximizing the agreement between embedding vectors from different views of the same image. A trivial solution is obtained when the encoder outputs constant vectors. This *collapse problem* is often avoided through implicit biases in the learning architecture, that often lack a clear justification or interpretation. In this paper, we introduce VICReg (Variance-Invariance-Covariance Regularization), a method that explicitly avoids the collapse problem with a simple regularization term on the variance of the embeddings along each dimension individually. VICReg combines the variance term with a decorrelation mechanism based on redundancy reduction and covariance regularization, and achieves results on par with the state of the art on several downstream tasks. In addition, we show that incorporating our new variance term into other methods helps stabilize the training and leads to performance improvements.

1 Introduction

Self-supervised representation learning has made significant progress over the last years, almost reaching the performance of supervised baselines on many downstream tasks [2, 33, 22, 40, 7, 21, 11, 49]. Several recent approaches rely on joint embedding learning with siamese networks [4], trained by maximising the agreement between different views of the same image. Contrastive methods [25, 22, 8] use a negative term that explicitly encourages the representations of different images to be different from each other. They rely on an expensive mining procedure of negative pairs which can be sampled from a memory bank [22] or from the current batch [8], followed by direct comparisons between the pairs. Although collapse is explicitly prevented, these methods are costly and require large batch sizes or memory banks. Alternatively, clustering based approaches [5, 7] force the representations to belong to different clusters, which also inherently prevents collapse, but still requires negative comparisons at the cluster level. Other successful methods do not rely on explicit strategies against collapsing solutions [21, 11] and are able to produce high-quality representations without any negative term or cluster assignment. They rely on asymmetric architectures and a discrepancy between the two siamese networks weights, which can be accomplished by using a momentum encoder [21, 37] or a stop-gradient operation [11]. These methods are efficient but are not well understood and rely on architectural tricks difficult to interpret. [41] provide a theoretical analysis and some insights on how collapse is avoided by asymmetric methods, but the complete dynamics is far from being understood and these methods might not work in other self-supervised learning setups. Finally, redundancy reduction methods [15, 49] avoid collapse by decorrelating the

Correspondence to abard@fb.com

dimensions of the representations, such that the representations are maximally informative about their corresponding input. This can be achieved by making the cross-correlation matrix of the features close to the identity matrix [49] or by whitening and scattering the features on the unit sphere [15]. These methods work well and are able to learn meaningful representations, while decorrelating them and maintaining their variance, all using one unique objective function. Our work propose to decompose these goals into three separate objective functions, each having a clear interpretation.

We introduce VICReg (Variance-Invariance-Covariance Regularization), a new self-supervised algorithm for learning image representations based on three simple principles, *variance*, *invariance* and *covariance* with clear objectives and interpretations. The variance principle constraints the variance of the embeddings along each dimension independently, and is a simple yet effective method against collapse. More precisely we use a hinge loss which constraints the standard deviation computed along the batch dimension of the embeddings to reach a fixed target. Unlike contrastive methods, no negative pairs are required and the embeddings are implicitly encouraged to be different from each other without any direct comparison between them. The invariance principle uses a standard mean-squared euclidean distance to learn invariance to multiple views of an image. Finally, the covariance principle borrows the covariance criterion of Barlow Twins [49], which decorrelates the different dimensions of the learned representations with the objective to spread the information across the dimensions, avoiding a *dimension collapse*. This criterion consists in penalizing the off-diagonal coefficients of the covariance matrix of the embeddings.

In SimCLR [8], the negative pairs are given by the batch, which implies a strong dependency to the batch size. We found no such dependency with our method. Similar to Barlow Twin [49], siamese weights discrepancy is not required either and our proposed architecture is symmetric, and works without the stop-gradient operation of SimSiam [11], the momentum encoder of BYOL [21] or the predictor used by both these methods. Unlike any previous self-supervised methods for representation learning [21, 11, 7, 49, 15], no form of normalization of the embeddings is required in the loss function, which keeps the method simple.

We demonstrate the effectiveness of our approach by evaluating the representations learnt with VICReg on many downstream tasks including the ImageNet [13] linear and semi-supervised evaluation protocols, and other classification, detection and instance segmentation tasks. We furthermore show that incorporating our variance regularization in more complicated architectures and other self-supervised representation learning methods lead to better training stability and performance improvement on downstream tasks. More generally, we show that VICReg is a simple yet effective and interpretable method for preventing collapse in self-supervised joint-embedding learning.

2 Related work

Contrastive learning. Discriminative self-supervised methods [14, 8] are based on direct comparison between training samples, and include contrastive methods where each sample in the dataset is considered as its own class [47, 25, 43, 35, 25, 22, 10, 33, 8, 9]. Most popular contrastive methods are based on the InfoNCE contrastive loss [35] which encourages representations from positive pairs of examples to be close in the embedding space while representations from negative pairs are pushed away from each other. Combined with siamese networks and joint embedding training, this approach is currently showing state of the art performance in self-supervised learning. However, contrastive methods require a large amount of negative pairs in order to work well. These negative pairs can be sampled from a memory bank as in MoCo [22], or given by the current batch of data as in SimCLR [8], with in both cases a large overhead in memory requirements. This downside of contrastive methods strongly motivates the needs for non-contrastive approaches.

Clustering methods. Instead of viewing each sample as its own class, clustering-based methods [3, 46, 44, 27, 51, 6, 1, 45, 18, 5, 7] regroup them into clusters based on some similarity measure. DeepCluster [5] uses k -means assignments of prior representations as pseudo-labels for the new representations which requires an expansive clustering phase, and makes the method hard to scale up. SwAV [7] mitigates this issue by learning the clusters online while maintaining a balanced partition of the assignments through the Sinkhorn-Knopp transform [12]. These clustering approaches can be viewed as contrastive learning at the level of clusters which still requires a lot of negative comparisons to work well.

Asymmetric networks methods. Recent work [11, 21, 37] has shown that it is possible to avoid the collapse problem while learning meaningful representations by using clever architectural tricks. These methods train an online network with learnable weights to predict the representations of a target network, for which the weights can be a moving average of the online network weights [21] or can be shared with the online network, but back-propagated only in the online branch of the siamese architecture, using a stop-gradient operation on the other side [11]. These methods are very powerful but suffer from a lack of explainability regarding the way collapsing solutions are avoided. In comparison, our solution explicitly prevents collapse, which might generalize better to various self-supervised learning scenarios where the networks do not share the same architecture.

Redundancy reduction methods. Whitening is a powerful operation for removing redundant information in some input data, it decorrelates the different variables and makes the variance of all variables identical. Inspired by [38], it has been used recently in self-supervised learning as a mechanism for preventing the dimensions of the representations from encoding the same information. W-MSE [15] performs a whitening operation via Cholesky decomposition and scatters the representations on the unit sphere, which requires inverting the covariance matrix of the embeddings and is therefore computationally expensive and unstable. Barlow Twins [49] makes the cross-correlation matrix of the representations close to the identity matrix, which forces strong correlations within each dimension of the representations between the two siamese branches, and decorrelates the pairs of different dimensions. Our method borrows this decorrelation mechanism but is completely free from normalization in its loss function and prevents collapse using its new variance regularization criterion.

3 Proposed method

The architecture of VICReg follows recent trends in self-supervised learning [8, 21, 7, 11, 49] and is based on joint embedding learning with siamese networks. As opposed to most previous work, the architecture is completely symmetric and consists of an encoder f_θ that outputs the final representations, followed by a projector h_ϕ that maps the representations into projections in an embedding space where the loss function will be computed. The role of the projector is to eliminate the low-level information in the representation that is not relevant for semantic comparison. The loss function uses an invariance term s that learns invariance to data transformations, and is regularized with a variance term v that prevents collapse and a covariance term c that decorrelates the different dimensions of the vectors. After pretraining, the projector is discarded and the representations of the encoder are used for downstream tasks.

More precisely, given an image $i \sim \mathcal{D}$ sampled from a dataset \mathcal{D} , two transformations t and t' are sampled from a distribution \mathcal{T} to produce two different views $x = t(i)$ and $x' = t'(i)$ of i . These transformations are random crops of the image, followed by color distortions. The distribution \mathcal{T} is described in Appendix B.2. The views are encoded using the encoder network f_θ into representations $y = f_\theta(x)$ and $y' = f_\theta(x')$. The representations are further processed by the projector h_ϕ into projections $z = h_\phi(y)$ and $z' = h_\phi(y')$. The loss is computed at the projection level on z and z' .

We describe here the variance, invariance and covariance terms that compose our loss function. The images are processed in batches, and we denote $Z = [z_1, \dots, z_n] \in \mathbb{R}^{n \times d}$ and $Z' = [z'_1, \dots, z'_n] \in \mathbb{R}^{n \times d}$ the two batches composed of n vectors of dimension d , of projections coming out of the two branches of the siamese architecture. We denote by Z_i the i^{th} vector in Z and $Z_{:,j}$ the vector composed of each value at dimension j in all vectors in Z . We define the variance regularization term v as a hinge loss on the standard deviation of the projections along the batch dimension:

$$v(Z) = \frac{1}{d} \sum_{j=1}^d \max(0, \gamma - \sqrt{\text{Var}(Z_{:,j}) + \epsilon}), \quad (1)$$

where γ is a target value for the standard deviation, fixed to 1 in our experiments, ϵ is a small scalar preventing numerical instabilities, and $\text{Var}(x)$ is the unbiased variance estimator given by:

$$\text{Var}(x) = \frac{1}{n-1} \sum_{i=1}^n (x_i - \bar{x})^2, \quad (2)$$

with n the size of x and \bar{x} the mean of x . This criterion will enforce the variance inside the current batch to be γ along each dimension, preventing collapsing solutions where all the inputs are mapped

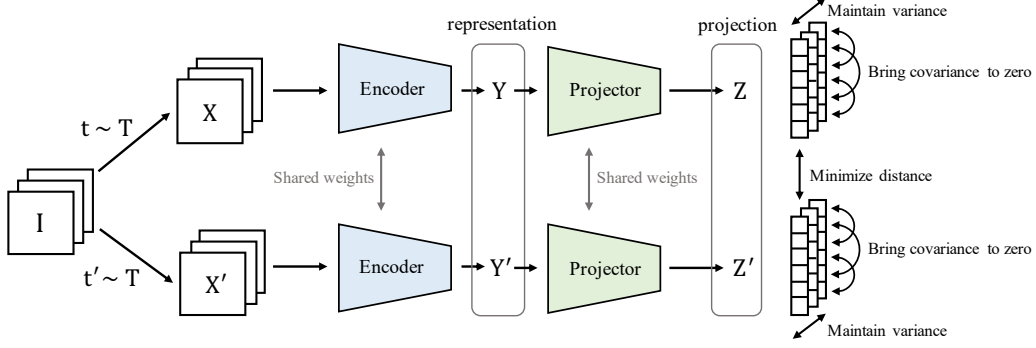


Figure 1: **VICReg: Siamese networks with variance, invariance and covariance regularization.** Given a batch of images I , two batches of different views X and X' are produced and are then encoded into representations Y and Y' . The representations are further processed into projections Z and Z' . The similarity between two projections from the same image is maximized, the variance along the batch dimension is maximized, while the different variables of the projections are progressively being decorrelated from each other.

to the same vector. Using the standard deviation and not directly the variance is crucial. Indeed, when the variance is used in the hinge loss, the gradient of the variance becomes very close to 0 when the input vector is close to its mean vector. The repulsive force of the hinge then becomes too small and the projections collapse. This is not the case with the standard deviation. We define the covariance matrix of Z as:

$$C(Z) = \frac{1}{n-1} \sum_{i=1}^n (Z_i - \bar{Z})(Z_i - \bar{Z})^T, \quad \text{where } \bar{Z} = \frac{1}{n} \sum_{i=1}^n Z_i. \quad (3)$$

Inspired by Barlow Twins [49], we can then define the covariance regularization term c as the sum of the squared off-diagonal coefficients of $C(Z)$, with a factor $1/d$ that scales the criterion as a function of the dimension:

$$c(Z) = \frac{1}{d} \sum_{i \neq j} C(Z)_{i,j}^2 \quad (4)$$

This term forces the off-diagonal coefficients to be close to 0, decorrelating the different dimensions of the projections and preventing these dimensions from encoding similar information. Decorrelation at the projection level ultimately has a decorrelation effect at the representation level, which is a none trivial phenomenon that we study in Appendix C.3. We finally define the invariance criterion s between Z and Z' as the mean-squared euclidean distance between each pair of vectors, the vectors of Z and Z' are not normalized either by standardization or by projection on the unit sphere:

$$s(Z, Z') = \frac{1}{n} \sum_i \|Z_i - Z'_i\|_2^2. \quad (5)$$

The overall loss function is a weighted average of the invariance, variance and covariance terms:

$$\ell(Z, Z') = \lambda s(Z, Z') + \mu \{v(Z) + v(Z')\} + \nu \{c(Z) + c(Z')\}, \quad (6)$$

where λ , μ and ν are hyper-parameters controlling the importance of each term in the loss. In our experiments we set $\nu = 1$ and perform an grid search study on the value of λ and μ with the base condition $\lambda = \mu > 1$, and set them to 25. The small value ϵ in Eq. (1) is set to 0.0001. The overall objective function taken on all images over an unlabelled dataset \mathcal{D} is given by:

$$\mathcal{L} = \sum_{I \in \mathcal{D}} \sum_{t, t' \sim \mathcal{T}} \ell(Z^I, Z'^I), \quad (7)$$

where Z^I and Z'^I are the batches of projection vectors corresponding to the batch of images I transformed by t and t' , and is minimized over the encoder parameters θ and projector parameters ϕ . We illustrate the architecture and loss function of VICReg in Figure 1.

Table 1: **Evaluation on ImageNet.** Evaluation of the learnt frozen representations from our pre-trained ResNet-50 backbone on (1) linear classification. (2) semi-supervised classification with 1% and 10% of the labels in the training set of ImageNet. We report Top-1 and Top-5 accuracies (in %).

Method	Linear Classification		Semi-supervised Classification			
	Top-1	Top-5	Top-1		Top-5	
			1%	10%	1%	10%
Supervised	76.5	-	25.4	56.4	48.4	80.4
MoCo [22]	60.6	-	-	-	-	-
PIRL [33]	63.6	-	-	-	57.2	83.8
CPC v2 [28]	63.8	-	-	-	-	-
CMC [39]	66.2	-	-	-	-	-
SimCLR [8]	69.3	89.0	48.3	65.6	75.5	87.8
MoCo v2 [10]	71.1	-	-	-	-	-
SimSiam [11]	71.3	-	-	-	-	-
SwAV [7]	71.8	-	-	-	-	-
InfoMin Aug [40]	73.0	91.1	-	-	-	-
BYOL [21]	74.3	91.6	53.2	68.8	78.4	89.0
SwAV (w/ multi-crop) [7]	75.3	-	53.9	70.2	78.5	89.9
Barlow Twins [49]	73.2	91.0	55.0	69.7	79.2	89.3
VICReg (ours)	73.2	91.1	54.8	69.5	79.4	89.5

4 Results

In this section we evaluate the representations obtained after self-supervised pretraining with VICReg. We train a ResNet-50 [24] backbone on the training set of the 1000-classes ImageNet ILSVRC-2012 dataset [13] without labels and evaluate it on the validation set of ImageNet on several vision and transfer learning tasks, including the linear evaluation protocol, the semi-supervised protocol, and other object detection and instance segmentation tasks.

4.1 Evaluation on ImageNet

Following the ImageNet [13] linear evaluation protocol, we train a linear classifier on top of the frozen representations of our ResNet-50 backbone pretrained with VICReg. We also evaluate the performance of the backbone when fine-tuned with a linear classifier on a subset of ImageNet’s training set using 1% or 10% of the labels, using the split of [8]. We compare in Table 1 our results on both tasks against other methods on the validation set of ImageNet. The performance of VICReg is on par with the state of the art without using the negative pairs of SimCLR, the clusters of SwAV, or any asymmetric networks architectural tricks such as the momentum encoder of BYOL and the stop-gradient operation of SimSiam. The performance is comparable with Barlow Twins performance, which shows that VICReg’s more explicit way of constraining the variance and comparing views has the same power than maximizing cross-correlations between pairs of twin dimensions. We give implementation details in Appendix B.3.

4.2 Transfer to other downstream tasks

Following the setup from [33], we train a linear classifier on top of the frozen representations learnt by our pretrained backbone, on a variety of different datasets: the Places205 [50] scene classification dataset, the VOC07 [16] multi-label image classification dataset and the INaturalist2018 [26] fine-grained image classification dataset. We then evaluate the quality of the representations by transferring to other vision tasks including VOC07+12 [16] and COCO [31] object detection using Faster R-CNN [36] with a R50-C4 backbone, and COCO [31] instance segmentation using Mask-RCNN [23] with a R50-FPN backbone. We report the performance in Table 2, VICReg performs on par with concurrent methods across all these tasks and datasets. We give implementation details in Appendix B.4.

Table 2: **Transfer learning on downstream tasks.** Evaluation of the learnt representations from our pretrained ResNet-50 backbone on (1) linear classification tasks on top of frozen representations, we report Top-1 accuracy (in %) for Places205 [50] and iNat18 [26], and mAP for VOC07 [16]. (2) Object detection with fine-tuning, we report AP₅₀ for VOC07+12 using Faster R-CNN with C4 backbone [36]. (3) Object detection and instance segmentation, we report AP for COCO [31] using Mask R-CNN with FPN backbone [23]. †: number from other methods run by us.

Method	Linear Classification			Object Detection		
	Places205	VOC07	iNat18	VOC07+12	COCO det	COCO seg
Supervised	53.2	87.5	46.7	81.3	39.0	35.4
MoCo [22]	46.9	79.8	31.5	-	-	-
PIRL [33]	49.8	81.1	34.1	-	-	-
SimCLR [8]	52.5	85.5	37.2	-	-	-
MoCo v2 [10]	51.8	86.4	38.6	82.5	39.8	36.1
SimSiam [11]	-	-	-	82.4	-	-
BYOL [21]	54.0	86.6	47.6	-	40.4 [†]	37.0 [†]
SwAV (w/ multi-crop) [7]	56.7	88.9	48.6	82.6	41.6	37.8
Barlow Twins [21]	54.1	86.2	46.5	82.6	40.0 [†]	36.7 [†]
VICReg (ours)	54.3	86.6	47.0	82.4	39.4	36.4

5 Ablations

In this section we study how the different components of our method contribute to its performance as well as how they interact with other components from other self-supervised methods. All reported results are obtained on the linear evaluation protocol using a ResNet-50 backbone and 100 epochs of pretraining, which gives results consistent with those obtained with 1000 epochs of pretraining. The optimization setting used for each experiment is described in Appendix B.5.

Asymmetric networks. We study the impact of different components used in asymmetric architectures and the effects of incorporating variance and covariance regularization into these architectures, in terms of performance and training stability. Starting from a simple symmetric architecture with an encoder and a projector without batch normalization, which correspond to VICReg without batch normalization in the projector, we progressively add batch normalization in the inner layers of the projector, a predictor, a stop-gradient operation and a momentum encoder. We use the training protocol and architecture of SimSiam [11] when a stop-gradient is used and the training protocol and architecture of BYOL [21] when a momentum encoder is used. The predictor as used in SimSiam and BYOL is a learnable module g_ψ that predicts the projection of a view given the projection of the other view of the same image. If z and z' are the projections of two views of an image, then $p = g_\psi(z)$ and $p' = g_\psi(z')$ are the predictions of each view. The invariance loss function of Eq. (5) is now computed between a batch of projections $Z = [z_1, \dots, z_n]$ and the corresponding batch of predictions $P = [p'_1, \dots, p'_n]$, and is symmetrized:

$$s(Z, Z', P, P') = \frac{1}{2n} \sum_i D(Z_i - P'_i) + \frac{1}{2n} \sum_i D(Z'_i - P_i), \quad (8)$$

where D is a distance function that depends on the method used. BYOL uses the mean square error between l_2 -normalized vectors, SimSiam uses the negative cosine similarity loss and VICReg uses the mean square error without l_2 -normalization. We compare different settings in Table 3, based on the default data augmentation, optimization and architecture settings of the original BYOL, SimSiam and VICReg methods. In VICReg, when a predictor is used, it has a similar architecture as the projector described in Appendix B.1, but with 2 layers instead of 3, which gives better results in practice. In all settings, the absence of BN indicates that BN is also removed in the predictor when one is used. The variance and covariance terms are computed on the batches of projections Z and Z' only, which we empirically found to work better than regularizing the output of the predictor.

We analyse first the impact of variance regularization (VR) in the different settings. When using VR, adding a predictor (PR) into VICReg does not lead to a significant change of the performance, which

Table 3: **The effect of incorporating variance and covariance regularization in different architectures.** Top-1 accuracy on the linear evaluation protocol with 100 pretraining epochs. 0.1% accuracy indicates collapsing of the representations. For all methods, pretraining follows the architecture, the optimization and the data augmentation protocol of the original method and is based on our implementation. ME: Momentum Encoder. SG: stop-gradient. PR: predictor. BN: Batch normalization layers after input and inner linear layers in the projector. No Reg: No additional regularization. Var Reg: Variance regularization. Var/Cov Reg: Variance and Covariance regularization. †: original method

Method	ME	SG	PR	BN	No Reg	Var Reg	Var/Cov Reg
BYOL	✓	✓	✓	✓	69.3 [†]	70.2	69.5
SimSiam		✓	✓	✓	67.9 [†]	68.1	67.6
SimSiam		✓	✓		35.1	67.3	67.1
SimSiam		✓			0.1	56.8	66.1
VICReg			✓		0.1	56.2	67.3
VICReg			✓	✓	0.1	57.1	68.7
VICReg				✓	0.1	57.5	68.6 [†]
VICReg					0.1	56.5	67.4

indicates that PR is redundant with VR. In comparison, without VR, the representations collapse, and stop-gradient (SG) and PR are both necessary, as the architecture needs to be asymmetric, as shown in [11]. Batch normalization in the inner layers of the projector (BN) leads to a 1.0% increase in the performance, which is not a big improvement considering that SG and PR without BN is performing very poorly at 35.1%. Finally incorporating VR with SG or ME further improves the performance by small margins of respectively 0.2% and 0.9%, which might be explained by the fact these architectural tricks that prevent collapse are not perfectly maintaining the variance of the representations to a strong threshold, i.e. very slow collapse is happening with these methods. We dive into this intuition by studying the evolution of the standard deviation of the representations during pretraining for BYOL and SimSiam in Appendix C.3. We then analyse the impact of adding additional covariance regularization (CR) in the different settings, along with variance regularization. We found that optimization with SG and CR is hard, even if our analysis of the average correlation coefficient of the representations during pretraining in Appendix C.3 shows that both fulfill the same objective. The performance of BYOL and SimSiam slightly drops compared to VR only, except when PR is removed, where SG becomes useless. BN is still useful and improves the performance by 1.3%. Finally with CR, PR does not harm the performance and even improves it by a very small margin. VICReg+PR with 1000 epochs of pretraining exactly matches the score of VICReg (73.2% on linear classification).

Batch size. Contrastive methods suffer from the need of a lot of negative examples which can translate into the need for very large batch sizes [8]. We study the performance on linear classification when the size of the batch varies between 128 and 4096. For each value of batch size, we perform a grid search on the base learning rate described in Appendix B.5. We observe a 0.7% and 1.2% drop in accuracy with small batch size of 256 and 128 which is comparable with the robustness to batch size of Barlow Twins [49] and SimSiam [11], and a 0.8% drop with a batch size of 4096, which is reasonable and allows our method to be very easily parallelized on multiple GPUs.

Batch size	128	256	512	1024	2048	4096
Top-1	67.3	67.9	68.2	68.3	68.6	67.8

Loss function coefficients. The loss function of VICReg is decomposed into 3 terms each having a clear objective. The invariance term learns invariance to multiple views of an image, the variance term prevents collapse and the covariance term decorrelates the different variables of the representations. We study here the importance of each term by setting either λ , μ or ν to 0 in Eq. (7), and report the

Table 4: **Ablation study.** Top-1 accuracy on linear classification with 100 pretraining epochs.

(a) **Impact of variance-covariance regularization.** Inv: a invariance loss is used, $\lambda > 0$, Var: variance regularization, $\mu > 0$, Cov: covariance regularization, $\nu > 0$, in Eq. (7).

Method	λ	μ	ν	Top-1
Inv	1	0	0	0.1
Inv + Cov	25	0	1	0.1
Inv + Cov	0	25	1	0.1
Inv + Var	1	1	0	57.5
Inv + Var + Cov (VICReg)	25	25	1	68.6

(b) **Impact of normalization.** Standardization: the projections are standardized. No BN in proj.: no batch normalization layer in the projector. l_2 -normalization: the projections are l_2 -normalized.

Method	Top-1
VICReg + Standardization	68.4
VICReg + Standardization + No BN in proj.	67.2
VICReg + No BN in proj.	67.4
VICReg + l_2 -normalization	65.1
VICReg	68.6

performance in Table 4a. Without variance regularization the representations immediately collapse to a single vector and the covariance term, which has no repulsive effect preventing collapse, has no impact. The invariance term is absolutely necessary and without it the network can not learn any good representations. By simply using the invariance term and variance regularization, which is a very simple baseline, we can still achieve an accuracy of 57.5%, which is only a 11.1% drop compared to the full method. These results show that variance and covariance regularization have complementary effects and fulfill very different objectives.

Normalizations. VICReg is the first self-supervised method free from any kind of normalization in its loss function that we are aware of. Contrary to SimSiam, W-MSE, SwAV and BYOL, the features are not projected on the unit sphere, and as opposed to Barlow Twins, they are not standardized (normalized with division by the standard deviation). We show in this subsection that no normalization is the optimal setting for VICReg. We study in Table 4b the impact of l_2 and batch normalization, in particular batch normalization at the end of the projector which plays the role of standardization.

When adding batch normalization at the end of the projector, the features are now standardized and the covariance matrix of Eq. (3) becomes the auto-correlation matrix with coefficients between -1 and 1, resulting in a drop by 1.1% of the performance. We observe that when unconstrained, the coefficients in the covariance matrix take values in a wider range, which gives more freedom to the network. Batch normalization is still an important component that helps stabilize the training when used in the inner layers of the projector, and the performance drops by 1.2% when it is completely removed.

Projecting the embeddings on the unit sphere constraints their standard deviation along the batch dimension to be $1/\sqrt{d}$, where d is the dimension of the vectors. We change the invariance term of Eq. (5) to be the cosine similarity:

$$s(Z, Z') = \frac{1}{n} \sum_i -\frac{1}{\|Z_i\|} Z_i \cdot \frac{1}{\|Z'_i\|_2} Z'_i, \quad (9)$$

and the target γ in the variance term of Eq. (1) is set to $1/\sqrt{d}$ instead of 1, enforcing the standard deviation to get closer to $1/\sqrt{d}$. This puts a lot more constraints on the network and the performance drops by 3.5%.

6 Discussion

In this section we compare VICReg with other methods in terms of methodology, and we discuss the mechanisms used by these methods to avoid collapse and to learn representations, and how they relate to VICReg.

Relation to Barlow Twins [49]. VICReg uses the same decorrelation mechanism as Barlow Twins, which consists in penalizing the off-diagonal terms of a covariance matrix computed on the projections. However, Barlow Twins uses the cross-correlation matrix where each entry in the matrix is a cross-correlation between two vectors $Z_{:,i}$ and $Z'_{:,j}$, from the two branches of the siamese architecture. Instead of using cross-correlations, we simply use the covariance matrix of each branch individually,

and the variance term of VICReg allows us to get rid of standardization. Indeed, Barlow Twins forces the correlations between pairs of vectors $Z_{:,i}$ and $Z'_{:,i}$ from the same dimension i to be 1. Without normalization, this target value of 1 becomes arbitrary and the vectors take values in a wider range. Moreover, there is an undesirable phenomenon happening in Barlow Twins, the embeddings before standardization can shrink and become constant to numerical precision, which could cause numerical instabilities and is solved by adding a constant scalar in the denominator of standardization. Without normalization, VICReg naturally avoids this edge case.

Relation to W-MSE [15] The whitening operation of W-MSE consists in computing the inverse covariance matrix of the projections and use its square root as a whitening operator on the projections. Using this operator has two downsides. First, matrix inversion is a very costly and unstable operation which requires a lot of care for the matrix to always be invertible. VICReg does not need to inverse the covariance matrix. Second, as mentioned in [15] the whitening operator is constructed over several consecutive iteration batches and therefore might have a high variance, which biases the estimation of the mean-squared error. This issue is overcome by a batch slicing strategy, where the whitening operator is computed over randomly constructed sub-batches. VICReg does not apply any operator on the projections, but instead regularizes the variance and covariance of the projections using an additional constraint.

Relation to BYOL and SimSiam [21, 11]. The core component that avoid collapse in BYOL and SimSiam is the stop-gradient operation on one side of their asymmetric architecture, which plays the role of the repulsive term used in other methods. Our experiments in Appendix C.3 show that in addition to prevent collapse, the stop-gradient operation also has a decorrelation effect, we observe in Figure 5 that even without covariance regularization, SimSiam and BYOL naturally minimize the average correlation coefficient of the representations. In addition, we make the following experiment, we compute the correlation matrix of the final representations obtained with SimSiam, BYOL, VICReg and VICReg without covariance regularization. We measure the average correlation coefficient and observe that this coefficient is much smaller for SimSiam, BYOL and VICReg, compared to VICReg without covariance regularization. VICReg replaces the stop-gradient operation, which is an architectural trick, by an explicit constraint on the variance and the covariance of the projections, which achieves the same goal of decorrelating the representations and avoiding collapse, while being clearer and more interpretable.

Relation to SimCLR and SwAV [8, 7]. Contrastive and clustering based self-supervised algorithms rely on direct comparisons between elements of negative pairs. In the case of SimCLR, the negative pairs involve embeddings mined from the current batch, and large batch sizes are required. Despite the fact that SwAV computes clusters using elements in the current batch, it does not seem to have the same dependency on batch size. However, it still requires a lot of prototype vectors for negative comparisons between embeddings and codes. VICReg eliminates these negative comparisons and replace them by an explicit constraint on the variance of the embeddings, which efficiently plays the role of a negative term between the vectors.

7 Conclusion

We have introduced VICReg, a simple approach to self-supervised image representation learning that decomposes the problem in three distinct principles, learning invariance to different views with a invariance term, avoiding collapse of the representations with a variance regularization term, and spreading the information throughout the different dimensions of the representations with a covariance regularization term. VICReg achieves results on par with the state of the art on many downstream tasks, pushing forward the boundaries of non-contrastive self-supervised learning.

The computational and memory complexity of VICReg are determined by the computation of the covariance matrix for each processed batch, which is quadratic in the dimension of the projection vectors. The experimental analysis of [49] and of VICReg has shown that increasing the dimension of the projections significantly improves the performance, which motivates the need for other redundancy reduction methods not based on the full computation of the covariance matrix. Future work will explore how this quadratic bottleneck can be overcome by different approximation techniques, as well as completely new redundancy reduction approaches based on higher-order statistics.

Acknowledgement. Jean Ponce was supported in part by the French government under management of Agence Nationale de la Recherche as part of the "Investissements d’avenir" program, reference ANR-19-P3IA-0001 (PRAIRIE 3IA Institute), the Louis Vuitton/ENS Chair in Artificial Intelligence and the Inria/NYU collaboration. Adrien Bardes was supported in part by a FAIR/Prairie CIFRE PhD Fellowship. The authors wish to thank Jure Zbontar for the BYOL implementation, Stéphane Deny for useful comments on the paper, and Li Jing, Yubei Chen, Mikael Henaff, Pascal Vincent and Geoffrey Zweig for useful discussions. We thank Quentin Duval and the VISSL team for help obtaining the results of table 2.

References

- [1] Asano, Y.M., Rupprecht, C., Vedaldi, A.: Self-labelling via simultaneous clustering and representation learning. In: ICLR (2020) 2
- [2] Bachman, P., Hjelm, R.D., Buchwalter, W.: Learning representations by maximizing mutual information across views. In: NeurIPS (2019) 1
- [3] Bautista, M.A., Sanakoyeu, A., Sutter, E., Ommer, B.: Cliqecnn: Deep unsupervised exemplar learning. In: NeurIPS (2016) 2
- [4] Bromley, J., Guyon, I., LeCun, Y., Sackinger, E., Shah, R.: Signature verification using a "siamese" time delay neural network. In: NeurIPS (1994) 1
- [5] Caron, M., Bojanowski, P., Joulin, A., Douze, M.: Deep clustering for unsupervised learning. In: ECCV (2018) 1, 2
- [6] Caron, M., Bojanowski, P., Mairal, J., Joulin, A.: Unsupervised pre-training of image features on non-curated data. In: ICCV (2019) 2
- [7] Caron, M., Misra, I., Mairal, J., Goyal, P., Bojanowski, P., Joulin, A.: Unsupervised learning of visual features by contrasting cluster assignments. In: NeurIPS (2020) 1, 2, 3, 5, 6, 9, 14, 15
- [8] Chen, T., Kornblith, S., Norouzi, M., Hinton, G.E.: A simple framework for contrastive learning of visual representations (2020) 1, 2, 3, 5, 6, 7, 9, 14
- [9] Chen, T., Kornblith, S., Swersky, K., Norouzi, M., Hinton, G.: Big self-supervised models are strong semi-supervised learners. In: NeurIPS (2020) 2
- [10] Chen, X., Fan, H., Girshick, R., He, K.: Improved baselines with momentum contrastive learning. arXiv preprint arXiv:2003.04297 (2020) 2, 5, 6
- [11] Chen, X., He, K.: Exploring simple siamese representation learning. In: CVPR (2020) 1, 2, 3, 5, 6, 7, 9, 14, 15, 16
- [12] Cuturi, M.: Sinkhorn distances: Lightspeed computation of optimal transport. In: NeurIPS (2013) 2
- [13] Deng, J., Dong, W., Socher, R., Li, L.J., Li, K., Fei-Fei, L.: Imagenet: A large-scale hierarchical image database (2009) 2, 5
- [14] Doersch, C., Gupta, A., Efros, A.A.: Unsupervised visual representation learning by context. In: ICCV (2015) 2
- [15] Ermolov, A., Siarohin, A., Sangineto, E., Sebe, N.: Whitening for self-supervised representation learning (2021) 1, 2, 3, 9
- [16] Everingham, M., Gool, L.V., Christopher K. I. Williams, J.W., Zisserman, A.: The pascal visual object classes (voc) challenge. IJCV (2010) 5, 6, 14
- [17] Fan, R.E., Chang, K.W., Hsieh, C.J., Wang, X.R., Lin, C.J.: Liblinear: A library for large linear classification. JMLR (2008) 14
- [18] Gidaris, S., Bursuc, A., Komodakis, N., Pérez, P., Cord, M.: Learning representations by predicting bags of visual words. In: CVPR (2020) 2
- [19] Goyal, P., Dollár, P., Girshick, R., Noordhuis, P., Wesolowski, L., Kyrola, A., Tulloch, A., Jia, Y., He, K.: Accurate, large minibatch sgd: Training imagenet in 1 hour. arXiv preprint arXiv:1706.02677 (2017) 13
- [20] Goyal, P., Duval, Q., Reizenstein, J., Leavitt, M., Xu, M., Lefaudeux, B., Singh, M., Reis, V., Caron, M., Bojanowski, P., Joulin, A., Misra, I.: Vissl. <https://github.com/facebookresearch/vissl> (2021) 14

- [21] Grill, J.B., Strub, F., Altché, F., Tallec, C., Richemond, P.H., Buchatskaya, E., Doersch, C., Pires, B.A., Guo, Z.D., Azar, M.G., Piot, B., Kavukcuoglu, K., Munos, R., Valko, M.: Bootstrap your own latent: A new approach to self-supervised learning. In: NeurIPS (2020) [1](#), [2](#), [3](#), [5](#), [6](#), [9](#), [13](#), [14](#), [15](#), [16](#)
- [22] He, K., Fan, H., Wu, Y., Xie, S., Girshick, R.: Momentum contrast for unsupervised visual representation learning. In: CVPR (2020) [1](#), [2](#), [5](#), [6](#), [14](#)
- [23] He, K., Gkioxari, G., Dollár, P., Girshick, R.: Mask r-cnn. In: ICCV (2017) [5](#), [6](#)
- [24] He, K., Zhang, X., Ren, S., Sun, J.: Deep residual learning for image recognition. In: CVPR (2016) [5](#), [13](#)
- [25] Hjelm, R.D., Fedorov, A., Lavoie-Marchildon, S., Grewal, K., Trischler, A., Bengio, Y.: Learning deep representations by mutual information estimation and maximization. In: ICLR (2019) [1](#), [2](#)
- [26] Horn, G.V., Aodha, O.M., Song, Y., Cui, Y., Sun, C., Shepard, A., Adam, H., Perona, P., Belongie, S.: The inaturalist species classification and detection dataset. In: CVPR (2018) [5](#), [6](#), [14](#)
- [27] Huang, J., and Shaogang Gong, Q.D., Zhu, X.: Unsupervised deep learning by neighbourhood discovery. In: ICML (2019) [2](#)
- [28] Hénaff, O.J., Srinivas, A., Fauw, J.D., Razavi, A., Doersch, C., Eslami, S.M.A., van den Oord, A.: Data-efficient image recognition with contrastive predictive coding. In: ICML (2019) [5](#)
- [29] Ioffe, S., Szegedy, C.: Batch normalization: Accelerating deep network training by reducing internal covariate shift. In: ICML (2015) [13](#)
- [30] Li, J., Zhou, P., Xiong, C., Hoi, S.C.: Prototypical contrastive learning of unsupervised representations. In: ICLR (2021) [15](#)
- [31] Lin, T.Y., Maire, M., Belongie, S., Bourdev, L., Girshick, R., Hays, J., Perona, P., Ramanan, D., Zitnick, C.L., Dollár, P.: Microsoft coco: Common objects in context. In: ECCV (2014) [5](#), [6](#)
- [32] Loshchilov, I., Hutter, F.: Sgdr: stochastic gradient descent with warm restarts. In: ICLR (2017) [13](#)
- [33] Misra, I., Maaten, L.v.d.: Self-supervised learning of pretext-invariant representations. In: CVPR (2020) [1](#), [2](#), [5](#), [6](#), [14](#)
- [34] Nair, V., Hinton, G.E.: Rectified linear units improve restricted boltzmann machines. In: ICML (2010) [13](#)
- [35] van den Oord, A., Li, Y., Vinyals, O.: Representation learning with contrastive predictive coding. arXiv preprint arXiv:1807.03748 (2018) [2](#)
- [36] Ren, S., He, K., Girshick, R., Sun, J.: Faster r-cnn: Towards real-time object detection with region proposal networks. In: NeurIPS (2015) [5](#), [6](#)
- [37] Richemond, P.H., Grill, J.B., Altché, F., Tallec, C., Strub, F., Brock, A., Smith, S., De, S., Pascanu, R., Piot, B., Valko, M.: Byol works even without batch statistics. arXiv preprint arXiv:2010.10241 (2020) [1](#), [3](#)
- [38] Siarohin, A., Sangineto, E., Sebe, N.: Whitening and coloring transform for gans. In: ICLR (2019) [3](#)
- [39] Tian, Y., Krishnan, D., , Isola, P.: Contrastive multiview coding. arXiv preprint arXiv:1906.05849v4 (2019) [5](#)
- [40] Tian, Y., Sun, C., Poole, B., Krishnan, D., Schmid, C., Isola, P.: What makes for good views for contrastive learning. In: NeurIPS (2020) [1](#), [5](#)
- [41] Tian, Y., Chen, X., Ganguli, S.: Understanding self-supervised learning dynamics without contrastive pairs. arXiv preprint arXiv:2102.06810 (2021) [1](#)
- [42] Wu, Y., Kirillov, A., Massa, F., Lo, W.Y., Girshick, R.: Detectron2. <https://github.com/facebookresearch/detectron2> (2019) [14](#)
- [43] Wu, Z., Xiong, Y., Yu, S., , Lin, D.: Unsupervised feature learning via non-parametric instance discrimination. In: CVPR (2018) [2](#), [15](#)

- [44] Xie, J., Girshick, R., Farhadi, A.: Unsupervised deep embedding for clustering analysis. In: ICML (2016) [2](#)
- [45] Yan, X., Misra, I., Gupta, A., Ghadiyaram, D., Mahajan, D.: Clusterfit: Improving generalization of visual representations. In: CVPR (2020) [2](#)
- [46] Yang, J., Parikh, D., Batra, D.: Joint unsupervised learning of deep representations and image clusters. In: CVPR (2016) [2](#)
- [47] Ye, M., Zhang, X., Yuen, P.C., Chang, S.F.: Unsupervised embedding learning via invariant and spreading instance feature. In: CVPR (2019) [2](#)
- [48] You, Y., Gitman, I., Ginsburg, B.: Large batch training of convolutional networks. In: arXiv preprint arXiv:1708.03888 (2017) [13](#), [15](#)
- [49] Zbontar, J., Jing, L., Misra, I., LeCun, Y., Deny, S.: Barlow twins: Self-supervised learning via redundancy reduction. arXiv preprint arxiv:2103.03230 (2021) [1](#), [2](#), [3](#), [4](#), [5](#), [7](#), [8](#), [9](#), [13](#), [14](#), [15](#)
- [50] Zhou, B., Lapedriza, A., Xiao, J., Torralba, A., Oliva, A.: Learning deep features for scene recognition using places database. In: NeurIPS (2014) [5](#), [6](#), [14](#)
- [51] Zhuang, C., Zhai, A.L., Yamins, D.: Local aggregation for unsupervised learning of visual embeddings. In: ICCV (2019) [2](#), [15](#)

A Algorithm

Algorithm 1 PyTorch-style pseudocode for VICReg.

```
# f: encoder network
# lambda, mu, nu: coefficients of the invariance, variance and
#   covariance losses
# N: batch size
# D: dimension of the representations
#
# mse_loss: Mean square error loss function
# off_diagonal: off-diagonal elements of a matrix
# relu: ReLU activation function

for x in loader: # load a batch with N samples
    # two randomly augmented versions of x
    x_a, x_b = augment(x)

    # compute representations
    z_a = f(x_a) # N x D
    z_b = f(x_b) # N x D

    # invariance loss
    sim_loss = mse_loss(z_a, z_b)

    # variance loss
    std_z_a = torch.sqrt(z_a.var(dim=0) + 1e-04)
    std_z_b = torch.sqrt(z_b.var(dim=0) + 1e-04)
    std_loss = torch.mean(relu(1 - std_z_a))
    std_loss = std_loss + torch.mean(relu(1 - std_z_b))

    # covariance loss
    z_a = z_a - z_a.mean(dim=0)
    z_b = z_b - z_b.mean(dim=0)
    cov_z_a = (z_a.T @ z_a) / (N - 1)
    cov_z_b = (z_b.T @ z_b) / (N - 1)
    cov_loss = off_diagonal(cov_z_a).pow_(2).sum() / D
    cov_loss = cov_loss + off_diagonal(cov_z_b).pow_(2).sum() / D

    # loss
    loss = lambda * sim_loss + mu * std_loss + nu * cov_loss

    # optimization step
    loss.backward()
    optimizer.step()
```

B Implementation details

B.1 Architecture and optimization

The encoder network f_θ of our architecture is a residual network [24] with 50 layers (ResNet-50) with 2048 output units. The projector h_ϕ is a multi-layer perceptron (MLP) with 3 layers, each inner layer followed with batch normalization (BN) [29] and a rectified linear unit (ReLU) [34]. Crucially, the last layer is not followed by neither BN nor ReLU. Similar to Barlow Twins we find that increasing the dimension of the inner and output layers of the projector is beneficial and we use 8192 inner and output units. We study the impact of the number of units in the layers of the projector in Appendix C.2. We follow the training procedure introduced in BYOL [21] and used in Barlow Twins [49]. We use the LARS optimizer [48, 19] and train the network for 1000 epochs with a weight decay of 10^{-6} and a learning rate $lr = batch_size / 256 \times base_lr$, where $batch_size$ is set to 2048 by default and $base_lr$ is a base learning rate set to 0.2. The learning rate follows a cosine decay schedule [32], starting from 0 with 10 warmup epochs and with final value of 0.002.

B.2 Data augmentation

We follow the image augmentation protocol first introduced in SimCLR [8] and now commonly used by similar approaches based on siamese networks [21, 7, 11, 49]. Two random crops from the input image are sampled and resized to 224×224 , followed by random horizontal flip, color jittering of brightness, contrast, saturation and hue, Gaussian blur and random grayscale. Each crop is normalized in each color channel using the ImageNet mean and standard deviation pixel values. In more details, the exact set of augmentations is based on BYOL [21] data augmentation pipeline but is symmetrised. The following operations are performed sequentially to produce each view:

- random cropping with an area uniformly sampled with size ratio between 0.2 to 1.0, followed by resizing to size 224×224 . `RandomResizedCrop(224, scale=(0.2, 0.1))` in PyTorch.
- random horizontal flip with probability 0.5
- color jittering of brightness, contrast, saturation and hue, with probability 0.8. `ColorJitter(0.4, 0.4, 0.2, 0.1)` in PyTorch.
- grayscale with probability 0.2
- gaussian blur with probability 0.5 and kernel size 23
- solarization with probability 0.1
- color normalization with mean (0.485, 0.456, 0.406) and standard deviation (0.229, 0.224, 0.225)

B.3 ImageNet evaluation

Linear evaluation. We follow standard procedure and train a linear classifier on top of the frozen representations of a ResNet-50 pretrained with VICReg. We use the SGD optimizer with a learning rate of 0.02, a weight decay of 10^{-6} , a batch size of 256, and train for 100 epochs. The learning rate follows a cosine decay. The training data augmentation pipeline is composed of random cropping and resize of ratio 0.2 to 1.0 with size 224×224 , and random horizontal flips. During evaluation the validation images are simply center cropped and resized to 224×224 .

Semi-supervised evaluation. We train a linear classifier and fine-tune the representations using 1 and 10% of the labels. We use the SGD optimizer with no weight decay a batch size of 256, and train for 20 epochs. In the 10% of labels case, we use a learning rate of 0.01 for the encoder and 0.1 for the linear head. In the 1% of labels case we use 0.03 for the encoder and 0.08 for the linear head. The two learning rates follow a cosine decay. The training data and validation augmentation pipelines are identical to the linear evaluation data augmentation pipelines.

B.4 Transfer learning

We use the VISSL library [20] for linear classification tasks and the detectron2 library [42] for object detection and segmentation tasks.

Linear classification. We follow standard protocols [33, 7, 49] and train linear models on top of the frozen representations. For VOC07 [16], we train a linear SVM with LIBLINEAR [17]. The images are center cropped and resized to 224×224 , and the C values are computed with cross-validation. For Places205 [50] we use SGD with a learning rate of 0.003, a weight decay of 0.0001, a momentum of 0.9 and a batch size of 256, for 28 epochs. The learning rate is divided by 10 at epochs 4, 8 and 12. For Inaturalist2018 [26], we use SGD with a learning rate of 0.005, a weight decay of 0.0001, a momentum of 0.9 and a batch size of 256, for 84 epochs. The learning rate is divided by 10 at epochs 24, 48 and 72.

Object detection and instance segmentation. Following the setup of [22, 49], we use the `trainval` split of VOC07+12 with 16K images for training and a Faster R-CNN C-4 backbone for 24K iterations with a batch size of 16. The backbone is initialized with our pretrained ResNet-50 backbone. We use a learning rate of 0.05, divided by 10 at iteration 18K and 22K and a linear warmup with slope of 0.333 for 1000 iterations. For COCO we use Mask R-CNN FPN backbone for 90K iterations with a batch size of 16, a learning rate of 0.04, divided by 10 at iteration 60K and 80K and with 50 warmup iterations.

Table 5: **K-NN classifiers on ImageNet.** Top-1 accuracy with 20 and 200 nearest neighbors.

Method	20-NN	200-NN
NPID [43]	-	46.5
LA [51]	-	49.4
PCL [30]	54.5	-
BYOL [21]	66.7	64.9
SwAV [7]	65.7	62.7
Barlow Twins [49]	64.8	62.9
VICReg	64.5	62.8

Table 6: **Impact of projector dimensionality.** Top-1 accuracy on the linear evaluation protocol with 100 pretraining epochs.

Dimensionality	256	512	1024	2048	4096	8192	16834
Top-1	55.9	59.2	62.4	65.1	67.3	69.1	69.3

B.5 Ablation studies

We give here implementation details on the results of Table 3, as well as the default setup for VICReg with 100 epochs of pretraining, used in all the other ablation tables. We use our own BYOL implementation in PyTorch, which outperforms the original implementation for 100 epochs of pretraining (69.3% accuracy on the linear evaluation protocol against 66.5% for the original implementation) and matches its performance for 1000 epochs of pretraining. We use the LARS optimizer [48], with a learning rate of $base_lr * batch_size / 256$ where $base_lr = 0.45$, and $batch_size = 4096$, a weight decay of 10^{-6} , an eta value of 0.001 and a momentum of 0.9, for 100 epoch of pretraining with 10 epochs of warmup. The learning rate follows a cosine decay schedule. The initial value of the exponential moving average factor is 0.99 and follows a cosine decay schedule. We use our own implementation of SimSiam, which reproduces exactly the performance reported in the paper [11]. We use SGD with a learning rate of $base_lr * batch_size / 256$ where $base_lr = 0.05$, $batch_size = 2048$, with a weight decay of 0.0001 and a momentum of 0.9 for 100 epochs of pretraining and 10 epochs of warmup. The learning rate of the encoder and the projector follow a cosine decay schedule while the learning rate of the predictor is kept fixed. For both BYOL and SimSiam experiments, the variance criterion has coefficient $\mu = 1$ and the covariance criterion has coefficient $\nu = 0.01$, the data augmentation pipeline and the architectures of the projector and predictor exactly follow the pipeline and architectures described in their paper. The setting of VICReg’s experiments is identical to the setting described in B.1, except that the number of pretraining epochs is 100 and the base learning rate is 0.3. The base learning rates used for the batch size study are 0.8, 0.5 and 0.4 for batch size 128, 256 and 512 respectively, and 0.3 for all other batch sizes. The linear evaluation setup of each methods follows closely the setup described in the original papers.

C Additional results

C.1 K-nearest-neighbors

Following recent protocols [43, 51, 7], we evaluate the learnt representations using K-nearest-neighbors classifiers built on the training set of ImageNet and evaluated on the validation set of ImageNet. We report the results with K=20 and K=200 in Table 5. VICReg performs slightly lower than other methods in the 20-NN case but remains competitive in the 200-NN case.

C.2 Projector network architecture

VICReg borrows the deccorelation mechanism of Barlow Twins [49] and we observe that it therefore has the same dependency to the dimensionality of the projector network. We study here the impact of the width and depth of the projector network. In the following table, the dimensionality corresponds

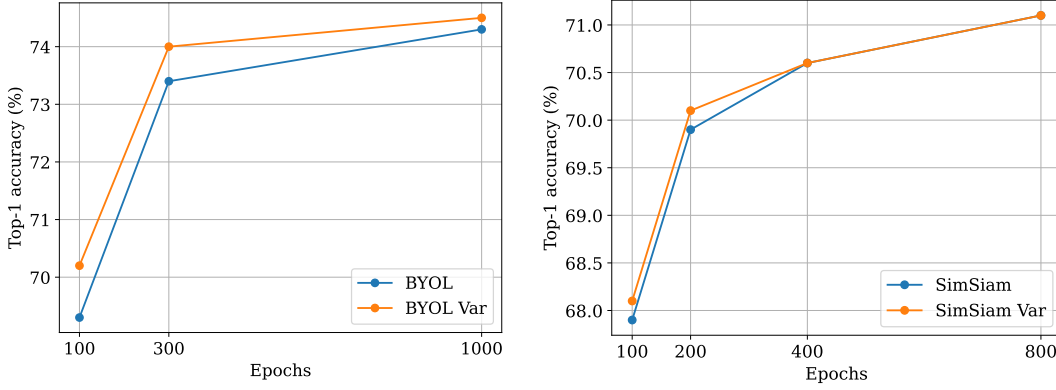


Figure 2: **Incorporating variance regularization in BYOL and SimSiam.** Top-1 accuracy on the linear evaluation protocol for different number of pretraining epochs. For both methods pre-training follows the optimization and data augmentation protocol of their original paper but is based on our implementation. *Var* indicates variance regularization

the number of hidden and output units in the projector network during pretraining. As the dimensionality increases, the performance dramatically increases from 55.9% top-1 accuracy on linear evaluation with a dimensionality of 256, to 69.3% with dimensionality 16384. The performance tends to saturate as the difference between dimensionality 8192 and 16384 is only of 0.2%.

C.3 Combination with BYOL and SimSiam

BYOL [21] and SimSiam [11] rely on a very unclear mechanism for preventing collapse, which leads to instabilities during the training. We incorporate our variance regularization loss into BYOL and SimSiam and show that it helps stabilize the training and offers a small performance improvement. For both methods, the results are obtained using our own implementation and the exact same data augmentation and optimization settings as in their original paper. The variance and covariance regularization losses are incorporated with a factor of $\mu = 1$ for variance and $\nu = 0.01$ for covariance. We report in Figure 2 the improvement obtained over these methods on the linear evaluation protocol for different number of pre-training epochs. For BYOL the improvement is of 0.9% with 100 epochs and becomes less significant as the number of pre-training epochs increases with a 0.2% improvement with 1000 epochs. This indicates that variance regularization makes BYOL converge faster. In SimSiam the improvement is not as significant. We plot in Figure 4 the evolution of the standard deviation computed along each dimension and averaged across the dimensions of the representation and the projections, during BYOL and SimSiam pretraining. For both methods, the standard deviation computed on the projections perfectly matches $1/\sqrt{d}$ where d is the dimension of the projections, which indicates that the projections are perfectly spread-out across the unit sphere. This translates in an increased standard deviation at the representation level, which seems to be correlated to the performance improvement. We finally study in Figure 5 the evolution of the average correlation coefficient, during pretraining of BYOL and SimSiam, with and without variance and covariance regularization. The average correlation coefficient is computed by averaging the off-diagonal coefficients of the correlation matrix of the representations:

$$\frac{1}{2d(d-1)} \sum_{i \neq j} C(Y)_{i,j}^2 + C(Y')_{i,j}^2, \quad (10)$$

where Y and Y' are the standardized representations and C is defined in Eq. (3). In BYOL this coefficient is much lower using covariance regularization, which translate in a small improvement of the performance, according to Table 3. We do not observe the same improvement in SimSiam, both in terms of correlation coefficient, and in terms of performance on linear classification. The average correlation coefficient is correlated with the performance, which motivates the fact that decorrelation and redundancy reduction is a core mechanism for learning self-supervised representations.

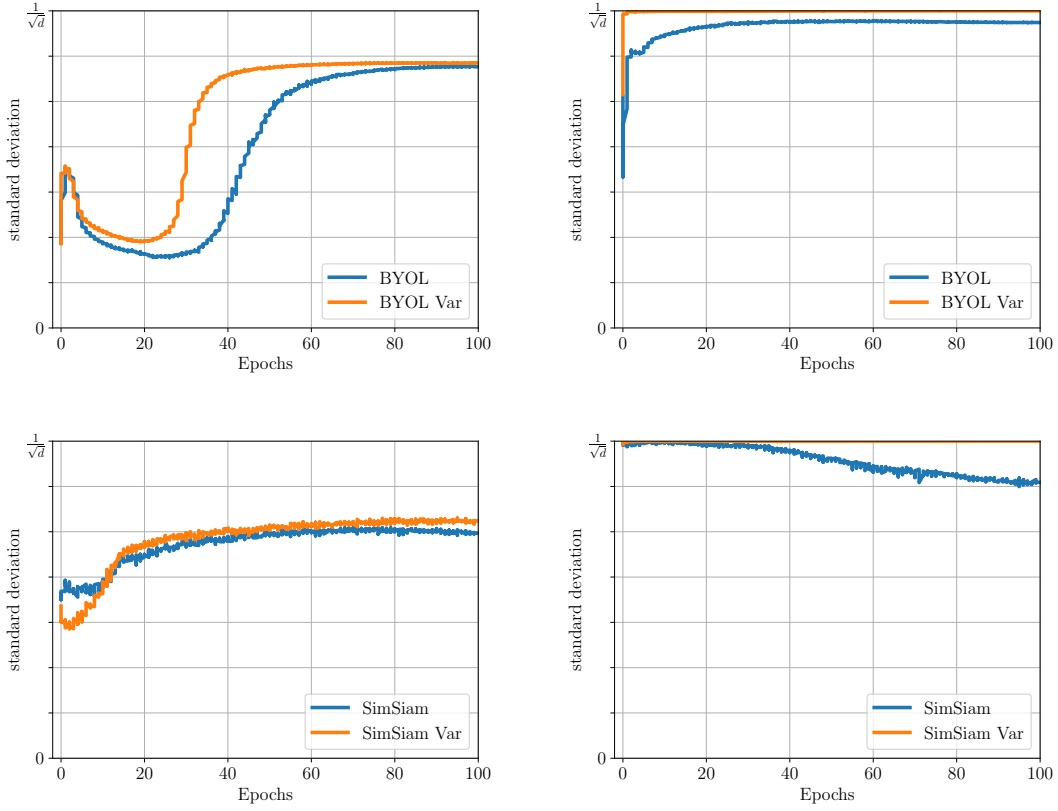


Figure 4: **Standard deviation of the features during BYOL and SimSiam pretraining.** Evolution of the average standard deviation of each dimension of the features with and without variance regularization (Var). left: the standard deviation is measured on the representations, right: the standard deviation is measured on the projections.

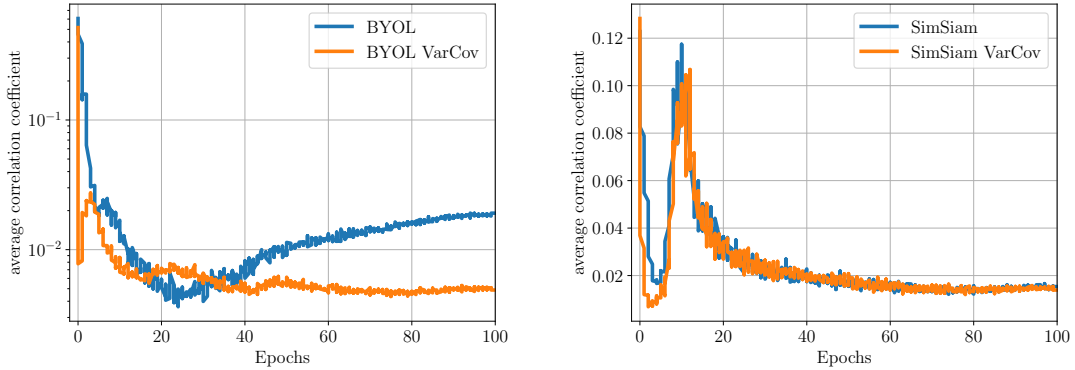


Figure 5: **Average correlation coefficient of the features during BYOL and SimSiam pretraining.** Evolution of the average correlation coefficient measured by averaging the off-diagonal terms of the correlation matrix of the representations with BYOL, BYOL with variance-covariance regularization (BYOL VarCov), SimSiam, and SimSiam with variance-covariance regularization (SimSiam VarCov).